Eur. J. Mech. B - Fluids 19 (2000) 123–137

Combined action of anticonvective and thermocapillary mechanisms of instability in multilayer systems

Ilya B. Simanovskii

Department of Mathematics, Technion—Israel Institute of Technology, 32000 Haifa, Israel

(Received 23 October 1998; revised 1 March 1999; accepted 2 June 1999)

Abstract – The nonlinear regimes of convection in the system of three immiscible viscous fluids heated from above are investigated. The interfaces are assumed to be flat. The boundary value problem is solved by the finite-difference method. Transitions between convective motions with different spatial structures are investigated. The common diagram of instability regimes is constructed. The new phenomena caused by direct and indirect interaction of anticonvective and thermocapillary mechanisms of instability are considered. Specifically, different oscillatory configurations where anticonvection arises mainly near the upper interface and thermocapillary convection appears mainly near the lower interface have been found. © 2000 Éditions scientifiques et médicales Elsevier SAS

1. Introduction

It is well known (Gershuni and Zhukhovitskii [1]) that in a horizontal fluid layer heated from above all the disturbances decay either in a monotonic or oscillatory manner and the mechanical equilibrium state is realized in the system. It was shown by Welander [2] that when the temperature gradient is directed vertically upwards, the two-layer system, consisting of two immiscible viscous fluids of infinite thicknesses, may become unstable with respect to the monotonic disturbances. The non-Rayleigh mechanism of instability (anticonvection) which is caused by heat and hydrodynamic interactions on the interface is realized in the system. It is important to emphasize that this specific mechanism of instability may appear only under the definite conditions: we must take fluids with considerably different physical properties. Particularly, the heat expansion coefficient of the upper layer must be much smaller than that of the lower layer, and the thermal diffusivity of the lower layer must be much higher than that of the upper one (or vice versa). The linear stability boundaries (for the layers of finite thickness) were determined by Gershuni and Zhukhovitskii [3] and the finite-amplitude regimes of anticonvection were obtained by Simanovskii [4] (see also Gershuni et al. [5]).

Another interfacial physical effect that may cause a convective instability is the thermocapillary effect which can generate stationary (Pearson [6]) and oscillatory motions (Sternling and Scriven [7], Palmer and Berg [8], Nepomnyashchy and Simanovskii [9]). In a real situation, various instability mechanisms may act simultaneously. The combined action of anticonvective and thermocapillary mechanisms of instability in a two-layer system was considered by Simanovskii [10] and Simanovskii et al. [11], where the steady convective motions with different spatial structures were obtained in the system. The three-layer systems can differ considerably from the systems with a single interface. The essentially new effect is the possibility of the interaction between two interfaces. In three-layer systems it is possible to speak about the direct interaction of anticonvective and thermocapillary mechanisms of instability (when both mechanisms act on one and the same interface) and indirect interaction (when both mechanisms act on different interfaces). Evidently, the last case cannot be realized in a two-layer system, and in this situation it is possible to expect the appearance of qualitatively new mechanisms of convective instabilities.

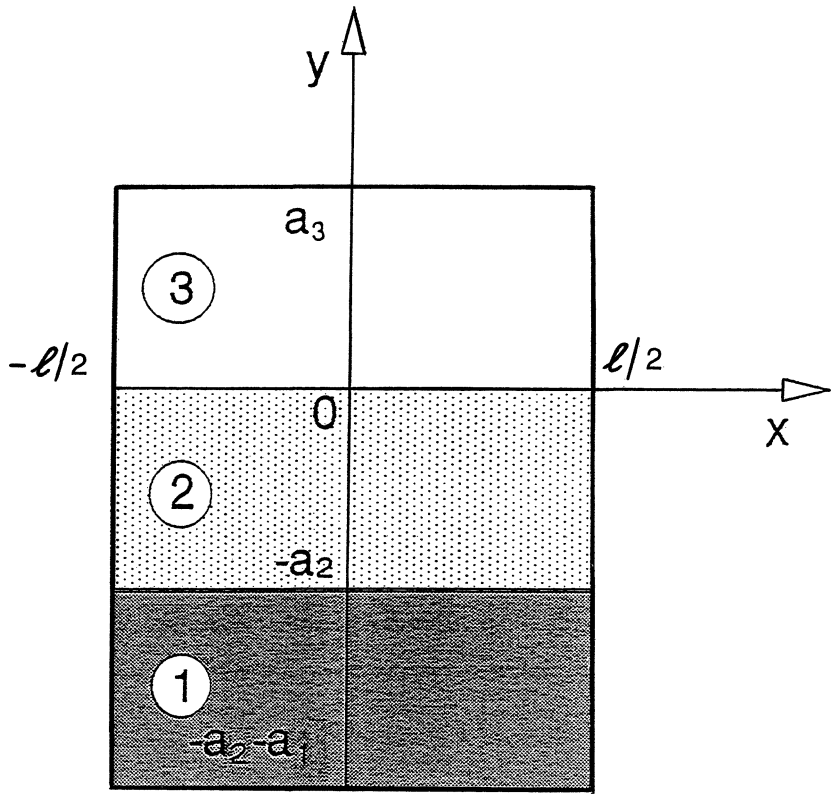

Figure 1. Geometrical configurations of the system and coordinate axes.

The investigation of multi-layer systems was started by Simanovskii et al. [12], Liu and Roux [13], Georis et al. [14], Georis [15] where the Marangoni–Benard and Rayleigh–Benard convection were considered. In these works for the system of three immiscible viscous fluids the linear stability of the mechanical equilibrium state and the non-linear convective motions were studied. Particularly, it was shown by Simanovskii et al. [12] and Georis et al. [14] that the three-layer system heated from below may become unstable with respect to oscillatory disturbances, and a new type of thermocapillary oscillations was discovered. During these oscillations both interfaces alternatively play the dominant role. Anticonvective mechanism of instability in a three-layer system was investigated by Simanovskii [16]; it was shown that in one and the same system anticonvection (for heating from above) and thermogravitational oscillations (for heating from below) can be realized.

In the present paper we consider the combined action of anticonvective and thermocapillary mechanisms of instability in three-layer systems with different physical properties. The paper is organized as follows. In Section 2 we describe the formulation of the problem and numerical method. Section 3 is devoted to consideration of the combined action of anticonvective and thermocapillary instability mechanisms. Section 4 contains some concluding remarks.

2. Formulation of the problem and the numerical method

Let a rectangular cavity with rigid boundaries be filled by three immiscible viscous fluids (see *figure 1*). Indices 1 and 3 are related to the exterior layers, and index 2 is related to the middle one. The plates are kept at

different constant temperatures (the total temperature drop is θ). It is assumed that surface tension coefficients on the upper and lower interfaces σ and σ_* decrease linearly with temperature: $\sigma = \sigma_0 - \alpha T$, $\sigma_* = \sigma_{0^*} - \alpha_* T$. The Boussinesq approximation is used for the description of convection. In the framework of the Boussinesq approximation, the deformations of the interfaces are negligible (Simanovskii and Nepomnyashchy [17]).

Let us use the following notations:

$$\nu_* = \nu_3/\nu_1, \qquad \nu = \nu_3/\nu_2, \qquad \eta_* = \eta_3/\eta_1, \qquad \eta = \eta_3/\eta_2, \qquad \kappa_* = \kappa_3/\kappa_1, \qquad \kappa = \kappa_3/\kappa_2,$$
$$\chi_* = \chi_3/\chi_1, \qquad \chi = \chi_3/\chi_2, \qquad \beta_* = \beta_3/\beta_1, \qquad \beta = \beta_3/\beta_2, \qquad \alpha = \alpha_*/\alpha,$$
$$a = a_1/a_3, \qquad a = a_2/a_3, \qquad L = l/a_3.$$

Here ν_i, η_i, κ_i, χ_i, β_i and a_i are, respectively, kinematic and dynamic viscosities, heat conductivity, thermal diffusivity, heat expansion coefficient and the thickness of the ith layer ($i = 1, 2, 3$). As the units of length, time, velocity, pressure and temperature we use a_3, a_3^2/ν_3, ν_3/a_3, $\rho_3\nu_3^2/a_3^2$ and θ, respectively. Introducing the stream function ψ and vorticity φ, we can write the dimensionless equations in the following form:

$$\begin{aligned}
&\frac{\partial \varphi_i}{\partial t} + \frac{\partial \psi_i}{\partial y}\cdot\frac{\partial \varphi_i}{\partial x} - \frac{\partial \psi_i}{\partial x}\cdot\frac{\partial \phi_i}{\partial y} = d_i \Delta\varphi_i + b_i G \frac{\partial T_i}{\partial x},\\
&\Delta\psi_i = -\varphi_i,\\
&\frac{\partial T_i}{\partial t} + \frac{\partial \psi_i}{\partial y}\cdot\frac{\partial T_i}{\partial x} - \frac{\partial \psi_i}{\partial x}\cdot\frac{\partial T_i}{\partial y} = \frac{c_i}{P}\Delta T_i \quad (i = 1, 2, 3).
\end{aligned} \tag{1}$$

Here, $d_3 = b_3 = c_3 = 1$; $d_1 = 1/\nu_*$, $b_1 = 1/\beta_*$, $c_1 = 1/\chi_*$; $d_2 = 1/\nu$, $b_2 = 1/\beta$, $c_2 = 1/\chi$; $G = g\beta_3\theta a_3^3/\nu_3^2$ is the Grashof number, $P = \nu_3/\chi_3$ is the Prandtl number for the liquid in layer 3.

At the interfaces, normal components of velocity vanish and the continuity conditions for tangential components of velocity and viscous stresses, temperatures and heat fluxes also apply:

$$\begin{aligned}
y = 0: \quad & \psi_2 = \psi_3 = 0, \quad \frac{\partial \psi_2}{\partial y} = \frac{\partial \psi_3}{\partial y}, \quad T_2 = T_3,\\
& \frac{1}{\kappa}\frac{\partial T_2}{\partial y} = \frac{\partial T_3}{\partial y}, \quad \eta\frac{\partial^2 \psi_3}{\partial y^2} = \frac{\partial^2 \psi_2}{\partial y^2} + Mr\frac{\partial T_3}{\partial x};
\end{aligned} \tag{2}$$

$$\begin{aligned}
y = -a: \quad & \psi_1 = \psi_2 = 0, \quad \frac{\partial \psi_1}{\partial y} = \frac{\partial \psi_2}{\partial y}, \quad T_1 = T_2,\\
& \frac{1}{\kappa_*}\frac{\partial T_1}{\partial y} = \frac{1}{\kappa}\frac{\partial T_2}{\partial y}, \quad \eta_*\eta^{-1}\frac{\partial^2 \psi_2}{\partial y^2} = \frac{\partial^2 \psi_1}{\partial y^2} + Mr_*\frac{\partial T_2}{\partial x}.
\end{aligned} \tag{3}$$

Here $Mr = \eta M/P$, $Mr_* = \eta_*\alpha M/P$; $M = \alpha\theta a_3/\eta_3\chi_3$ is the Marangoni number. On the horizontal solid plates the boundary conditions have the form:

$$y = 1: \quad \psi_3 = \frac{\partial \psi_3}{\partial y} = 0, \quad T_3 = 0; \tag{4}$$

$$y = -a - a_*: \quad \psi_1 = \frac{\partial \psi_1}{\partial y} = 0, \quad T_1 = -1 \tag{5}$$

(as the reference point for the temperature we choose the temperature on the upper rigid plate).

We consider the following boundary conditions on vertical walls:

$$x = -L/2, L/2: \quad \psi_i = \frac{\partial \psi_i}{\partial x} = 0, \quad \frac{\partial T_i}{\partial x} = 0, \quad i = 1, 2, 3. \tag{6}$$

The boundary value problem (1)–(6) contains seventeen independent non-dimensional parameters. The parametric investigation of this problem seems to be impossible. Because of this we shall concentrate on some particular systems of fluids demonstrating various characteristic phenomena.

The boundary value problem (1)–(6) was solved by the finite difference method. Equations were approximated on a uniform 28×84 mesh using a second order approximation for the spatial coordinates and solved using an explicit scheme with central differences. The time step was calculated by the formula:

$$\Delta t = \frac{[\min(\Delta x, \Delta y)]^2 \times [\min(1, \nu, \chi, \nu_*, \chi_*)]}{2[2 + \max \psi_i(x, y)]}.$$

The Poisson equations were solved by the iterative Liebman successive over-relaxation method on each time step. It turned out that the oscillatory motions were more sensitive to the numerical inaccuracies. Because of that, we used a more accurate solution of the Poisson equations in the oscillatory case. Actually, the quantity

$$\varepsilon = \max \frac{|(\psi_i)^{n+1} - (\psi_i)^n|}{|(\psi_i)^n|},$$

where n is the number of iterations, was smaller than 10^{-4} for steady solutions and 10^{-5} for oscillations. The Kuskova and Chudov formulas (Kuskova and Chudov [18]) providing the second order accuracy were used for approximation of the vorticity on the solid boundaries. For example, on the boundary $x = -L/2$:

$$\varphi_i(-L/2, y) = \frac{\psi_i(2\Delta x, y) - 8\psi_i(\Delta x, y)}{2(\Delta x)^2}.$$

At the interfaces the expressions for the vorticities at the exterior layers were approximated with a second-order scheme for the spatial coordinates and had a form:

$$\varphi_3(x, 0) = -\frac{2[\psi_2(x, -\Delta y) + \psi_3(x, \Delta y)]}{(\Delta y)^2(1 + \eta)} - Mr \frac{1}{1 + \eta} \frac{\partial T_3}{\partial x}(x, 0), \tag{7}$$

$$\varphi_2(x, 0) = \eta \varphi_3(x, 0) + Mr \frac{\partial T_3}{\partial x}(x, 0), \tag{8}$$

$$\varphi_2(x, -a) = -\frac{2[\psi_1(x, -a - \Delta y) + \psi_2(x, -a + \Delta y)]}{(\Delta y)^2(1 + \eta_* \eta^{-1})} - Mr_* \frac{1}{1 + \eta_* \eta^{-1}} \frac{\partial T_2}{\partial x}(x, -a), \tag{9}$$

$$\varphi_1(x, -a) = \eta_* \eta^{-1} \varphi_2(x, -a) + Mr_* \frac{\partial T_2}{\partial x}(x, -a). \tag{10}$$

Here Δx, Δy are the mesh sizes for the corresponding coordinates. The temperatures on the interfaces were calculated by the second-order approximation formulas:

$$T_2(x, 0) = T_3(x, 0) = \frac{[4T_2(x, -\Delta y) - T_2(x, -2\Delta y)] + \kappa[4T_3(x, \Delta y) - T_3(x, -2\Delta y)]}{3(1 + \kappa)},$$

Table I. Dependence of τ and $(\psi_3)_{\max}$ on mesh size.

Mesh sizes	τ	$(\psi_3)_{\max}$
28×84	0.992	3.128
42×84	0.992	3.154
28×126	0.992	3.140
56×168	0.992	3.195

Table II. Dependence of τ and $(\psi_3)_{\max}$ on time step.

Time step	τ	$(\psi_3)_{\max}$
Δt	0.992	3.128
$\Delta t/2$	0.992	3.121
$\Delta t/4$	0.992	3.117

$$T_2(x,-a) = T_1(x,-a) = \frac{\kappa_*[4T_2(x,-a+\Delta y) - T_2(x,-a+2\Delta y)] + \kappa[4T_1(x,-a-\Delta y) - T_1(x,-a-2\Delta y)]}{3(\kappa+\kappa_*)}.$$

The same code was formerly used for calculation of convective flows in three-layer systems (see Simanovskii et al. [12], Georis et al. [14]). It turned out to be efficient for calculation of both stationary and oscillatory convective motions.

To estimate the accuracy of the results, we performed some tests. We checked up the results on 42×84, 28×126 and 56×168 meshes. The typical test results obtained for the system described in Section 3.2 ($M = 27500$, $G = 4500$, $\alpha = 200$) are shown in *tables I* and *II*. These tables present the dependences of the oscillations period τ and the maximal value of the stream function $(\psi_3)_{\max}$ in the upper layer on the mesh size (*table I*) and time step (*table II*). Relative changes of stream function amplitudes for all mesh sizes do not exceed 3%. The maximal relative changes (up to 12%) were observed for the vorticity near the corner points where the vorticity field is not continuous. The details of the numerical method can be found in the book of Simanovskii and Nepomnyashchy [17].

3. Interaction on anticonvection and thermocapillarity—numerical results

3.1. Direct interaction

Let us consider the model system heated from above which is characterized by the following set of parameters: $\eta = 0.2$, $\nu = 1$, $\kappa = 0.1$, $\chi = 0.1$, $\beta = 0.01$, $\eta_* = 0.04$, $\nu_* = 1$, $\kappa_* = 0.1$, $\chi_* = 0.07$, $\beta_* = 0.01$, $\alpha = 1$, $a = a_* = 1$. It means that the heat expansion coefficient of the upper layer is much smaller than that of the middle layer, and the thermal diffusivity of the middle layer is much higher than that of the upper one. The values of the Prandtl number and the ratio of the length of the cavity to the thickness of the upper layer are fixed: $P = 1$, $L = 2.5$. This choice is based on the fact that this system displays an anticonvective instability (Simanovskii [16]). The explanation of the physical nature of the anticonvective instability mechanism, given by Gershuni and Zhukhovitskii [3] (see also Simanovskii [16]), is as follows.

The temperature fluctuation at the upper interface generates convection in the middle fluid with high buoyancy. This convective motion cannot neutralize the temperature fluctuation due to the high thermal diffusivity of the middle layer. At the same time, the convective motion in the middle layer provides the

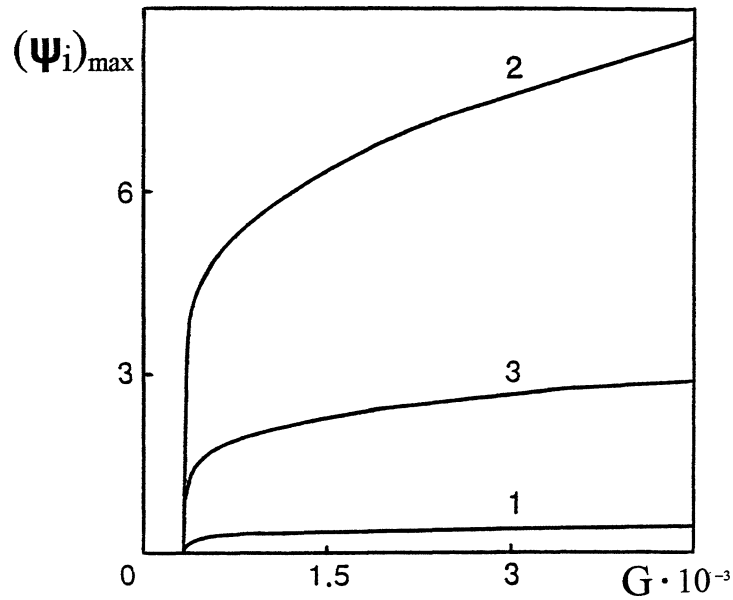

Figure 2. Dependence of maximum values of stream function modulus $(\psi_i)_{\max}$ $(i = 1, 2, 3)$ on the Grashof number $(\alpha = 1)$.

viscous stresses, that induce a motion in the upper fluid with the weak buoyancy. The latter motion supports the temperature fluctuation.

With the increase in the Grashof number, the mechanical equilibrium state becomes unstable and the steady motion is realized in the system as $G_* \geqslant 2900$. For the system under consideration, conditions for the appearance of the anticonvection (as $G \neq 0$, $M = 0$) are satisfied on the upper interface. Therefore, the anticonvection is generated in the upper layer and in the middle layer. Among these two layers, the intensity of the convection, as usual, is higher in the layer with higher buoyancy, e.g. in the middle layer (see *figure 2*). The motion in the lower layer is induced by viscous stresses on the lower interface, and its intensity is relatively low (see *figure 2*). The typical structures of the anticonvective motion for different values of the Grashof numbers are shown in *figures 3(a)* and *3(b)*. The stream function and the temperature fields have the symmetry

$$\psi_i(-x, y) = -\psi_i(x, y), \quad T_i(-x, y) = T_i(x, y) \quad (i = 1, 2, 3). \tag{11}$$

Close to the instability threshold an additional vortex appears in the third layer near the upper interface (see *figure 3(a)*). At the larger values of G the intensity of convection grows and the additional vortex becomes comparable in volume (but not in intensity) with the main one (see *figure 3(b)*). The above conclusions are not sensitive to the numerical inaccuracies. Near the lower interface a weak motion exists.

The thermocapillary convection ($M \neq 0$, $G = 0$) also appears near the upper interface. Unlike the case of anticonvection, the intensities of the thermocapillary convection in both upper and middle layers are of the same order (see *figure 4*). The directions of rotation coincide for anticonvective and thermocapillary motions. When both mechanisms of instability act simultaneously, the intensity of the motion increases in both fluids, but its increase in the middle layer is much stronger (see *figure 5*).

Thus, for the given system the direct interaction of both mechanisms of instability does not produce qualitatively new flow structures.

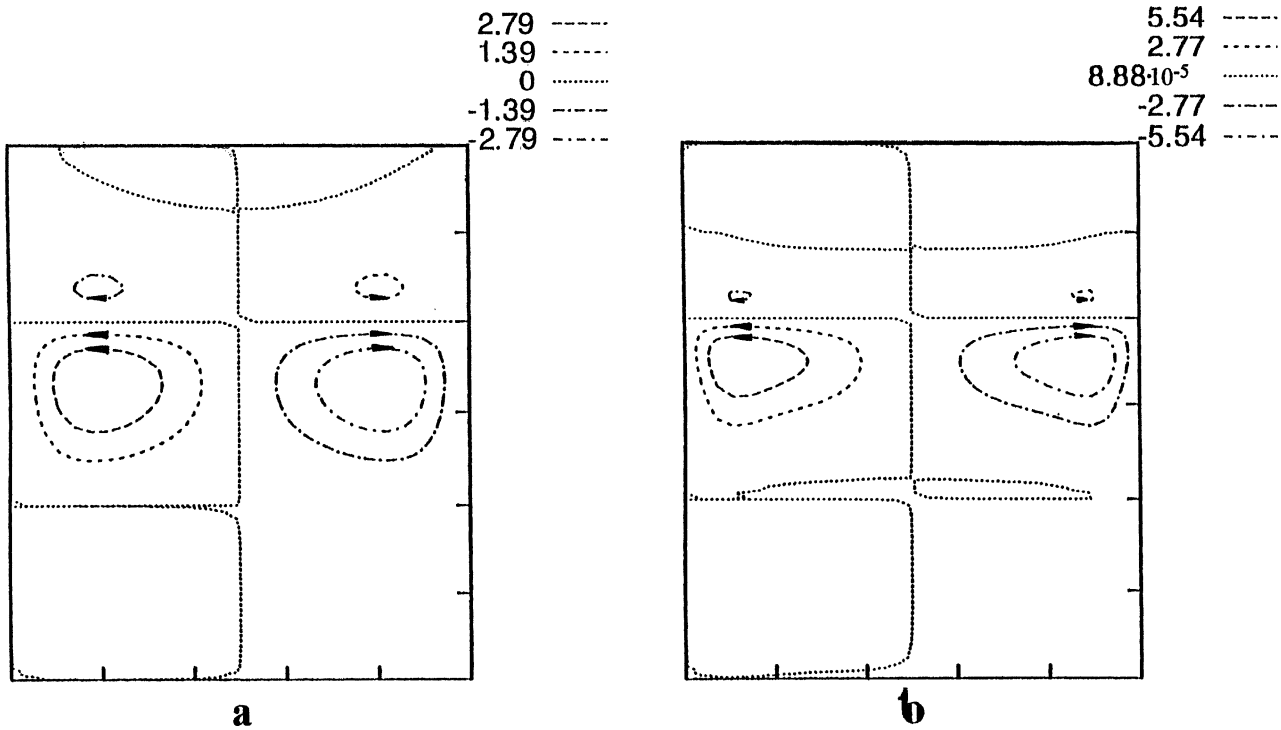

Figure 3. Streamlines for the steady motion ($M = 0$): (a) $G = 4500$; (b) $G = 42000$.

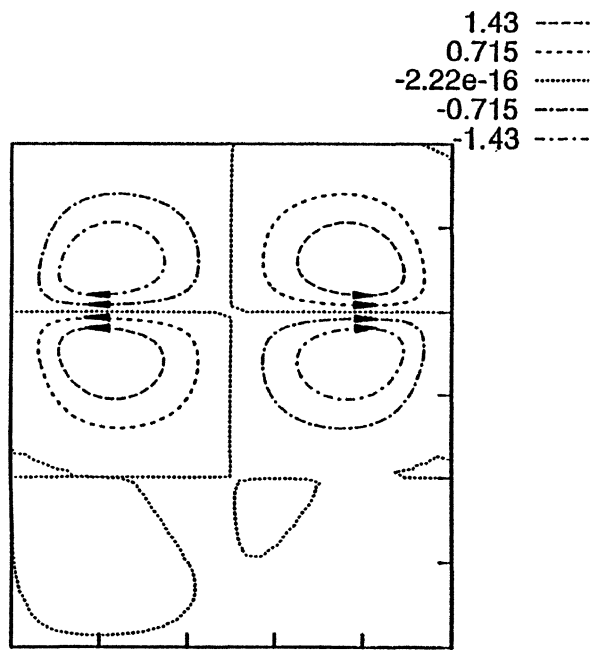

Figure 4. Streamlines for pure thermocapillary motion ($M = 12000$, $G = 0$, $\alpha = 1$).

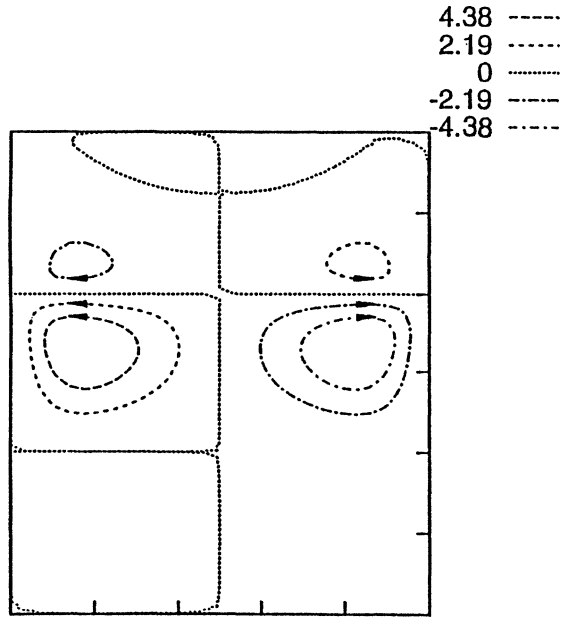

Figure 5. Streamlines for the combined action of thermocapillary and anticonvective mechanisms of instability ($M = 12000$, $G = 4500$, $\alpha = 1$).

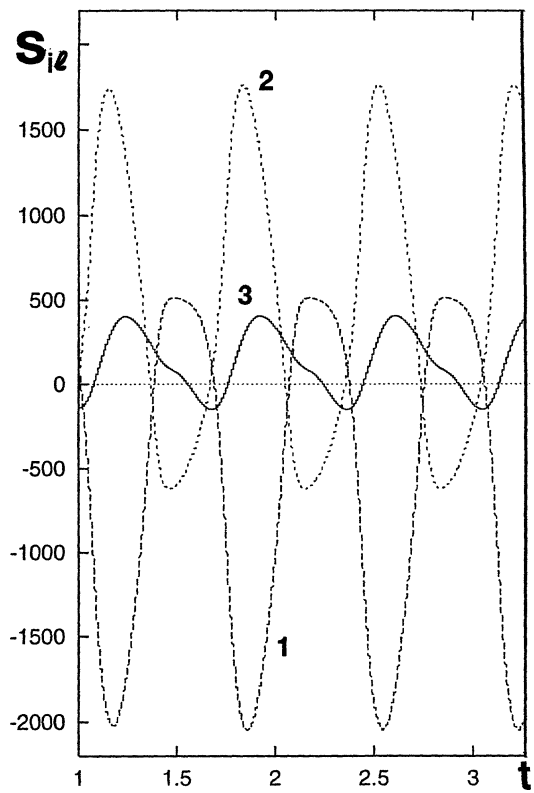

Figure 6. The dependence $S_{il}(t)$ $(i = 1, 2, 3)$ for $M = 8500$, $G = 0$, $\alpha = 200$.

3.2. Indirect interaction

In the present subsection, we shall concentrate on a qualitatively new situation, where both instability mechanisms act on different interfaces. Such an 'indirect' interaction of instability mechanisms is possible only in three-layer systems. With the change in α (all the other parameters being the same), the role of two interfaces in the generation of the thermocapillary convection ($M \neq 0$, $G = 0$) also changes. If $1 < \alpha < 180$ thermocapillary convection is generated by both interfaces, and if $\alpha > 180$, the thermocapillary motion takes place mainly near the lower interface. We shall take the previous system with $\alpha = 200$. When the Marangoni number is small enough, the system keeps the mechanical equilibrium state; all the disturbances decay in an oscillatory manner. With the increase in M the mechanical equilibrium state becomes unstable and the oscillatory motion is realized in the system.

To simplify the description of motions, we shall introduce the following integral characteristics:

$$
\begin{aligned}
S_{1l}(t) &= \int_{-L/2}^{0} dx \int_{-a-a_*}^{-a} dy\, \psi_1(x, y, t),\\
S_{2l}(t) &= \int_{-L/2}^{0} dx \int_{-a}^{0} dy\, \psi_2(x, y, t),\\
S_{3l}(t) &= \int_{-L/2}^{0} dx \int_{0}^{1} dy\, \psi_3(x, y, t), \qquad S_{3r}(t) = \int_{0}^{L/2} dx \int_{0}^{1} dy\, \psi_3(x, y, t).
\end{aligned}
\tag{12}
$$

that provide some reduced information about the intensity and the symmetry of the motion.

Not far from the threshold, oscillations have a rather simple, almost sinusoidal form (see *figure 6*), but the mean values of $S_{il}(t)$, $i = 1, 2, 3$ are different from zero. The fields of stream function and temperature do not

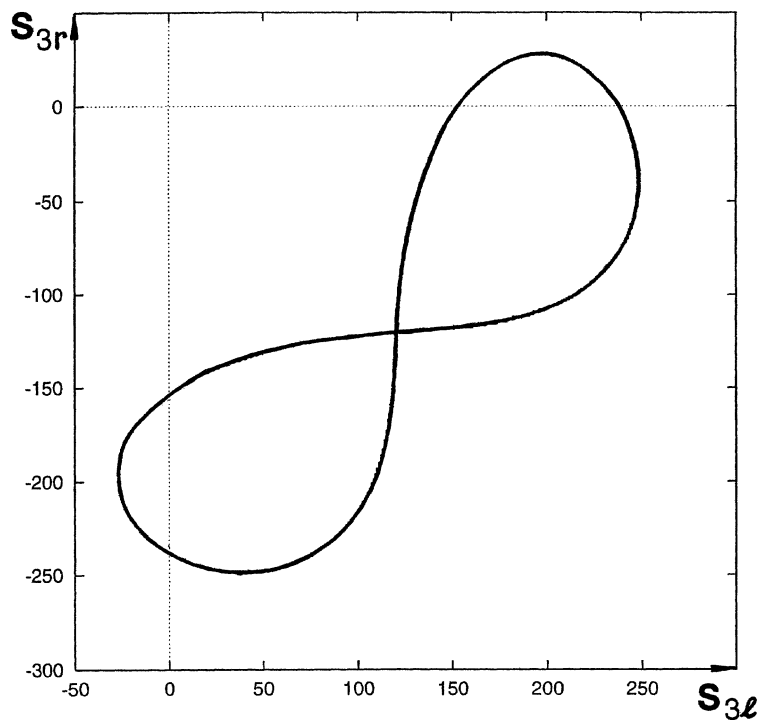

Figure 7. The phase trajectory for thermocapillary motion ($M = 8500$, $G = 0$, $\alpha = 200$).

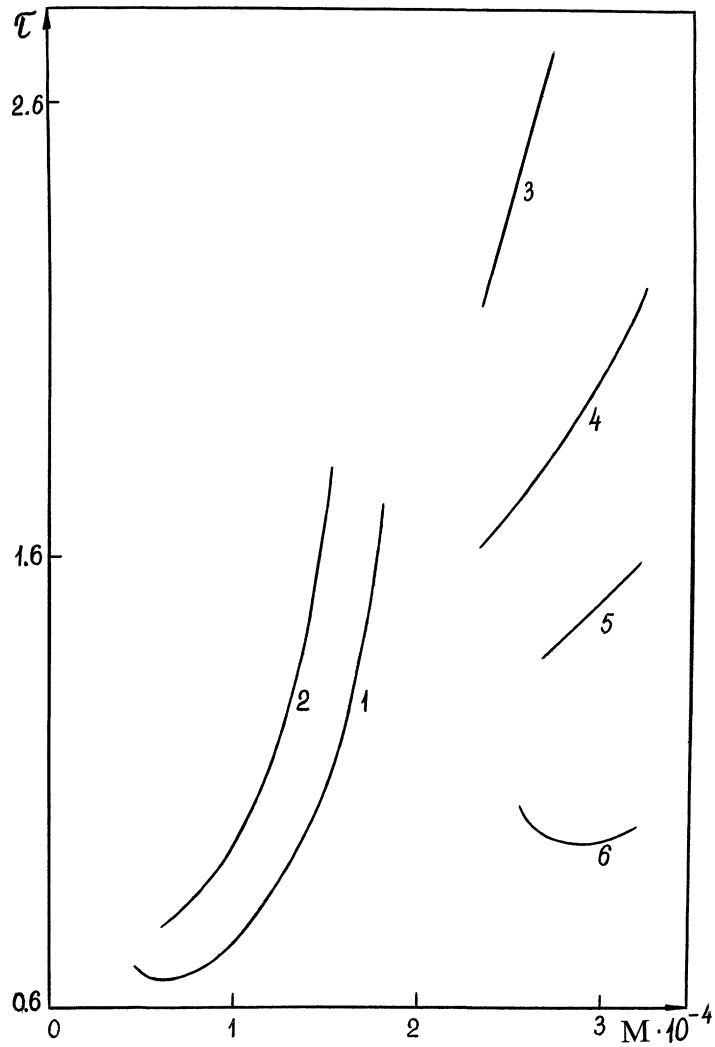

Figure 8. The dependence of the period of oscillations on the Marangoni number: (1) $G = 0$; (2) $G = 250$; (3) $G = 3250$; (4) $G = 3500$; (5) $G = 3750$; (6) $G = 4500$.

satisfy the symmetry conditions (11). The typical phase trajectory is presented in *figure 7*. With the increase in the Marangoni number, the period of oscillations grows (see *figure 8*, line 1). For $M > 17500$ oscillations become unstable and the steady motion is realized in the system. The streamlines, corresponding to this steady state, are presented in *figure 9*. Thus, for the given system the thermocapillary motion ($M \neq 0$, $G = 0$) takes place mainly near the lower interface.

Let us consider now the combined action of both mechanisms of instability. We shall remind, that the upper interface plays an active role in the generation of anticonvection if $G \neq 0$, $M = 0$. The common diagram of instability regimes on the plane "the Grashof number–the Marangoni number" is shown in *figure 10*. One can see that inclusion of G leads to the destruction of oscillations of the thermocapillary nature (see *figure 10*, region I) and establishment of the steady state in the system. The typical structure of the steady motion at the relatively small values of G and M is shown in *figure 11*. At the larger values of M and G the new type of oscillations, essentially connected with the indirect interaction of both mechanisms of instability is

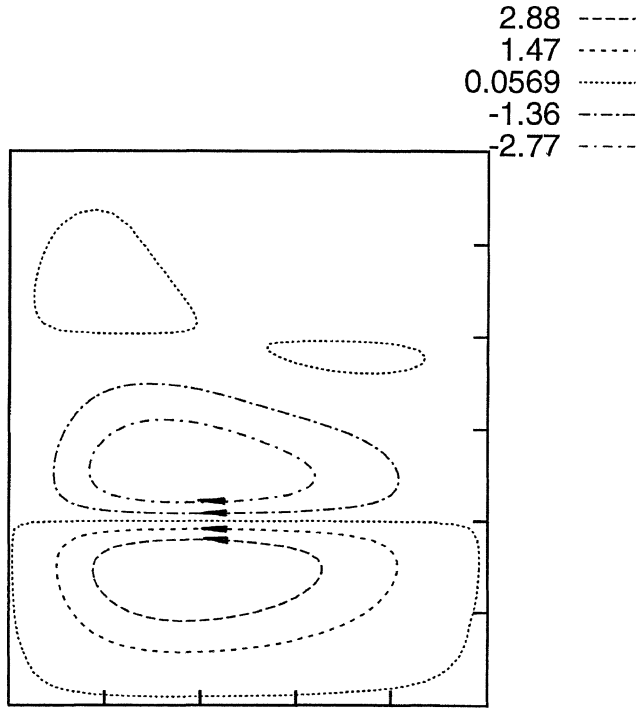

Figure 9. Streamlines for the steady state ($M = 20000$, $G = 0$, $\alpha = 200$).

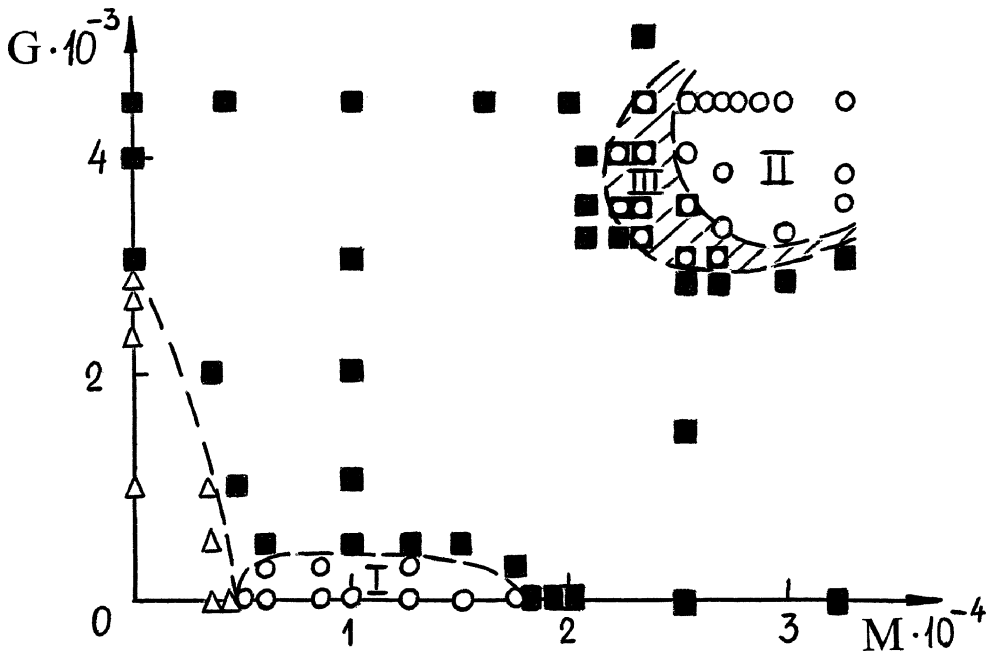

Figure 10. The common diagram of instability regimes on the plane "the Marangoni number–the Grashof number" ((△) equilibrium state; (■) steady state; (○) oscillations; the dashed region—overlapping of the stability regions of the steady state and oscillations).

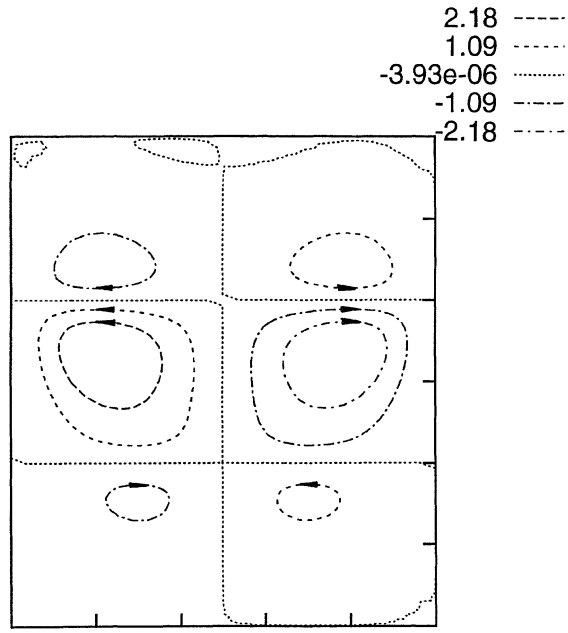

Figure 11. Streamlines for the steady state ($M = 10000$, $G = 2000$, $\alpha = 200$).

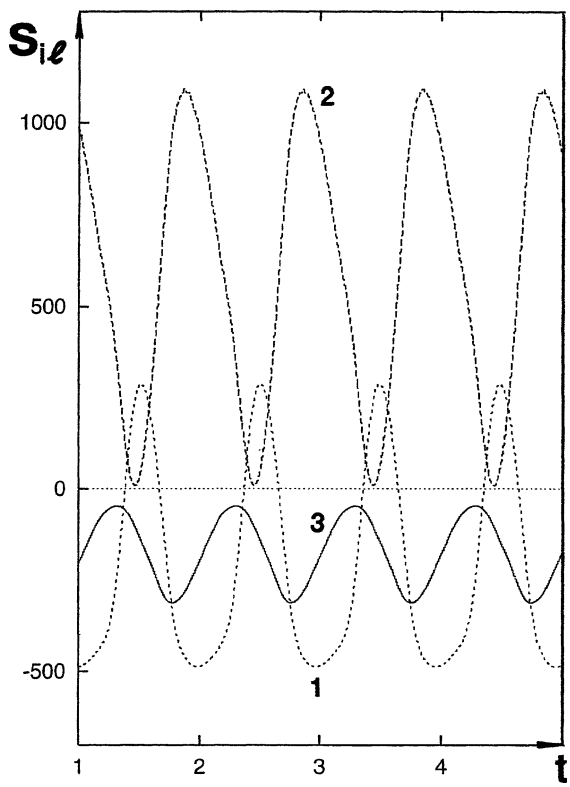

Figure 12. The dependence $S_{il}(t)$ $(i = 1, 2, 3)$ for $M = 27500$, $G = 4500$, $\alpha = 200$.

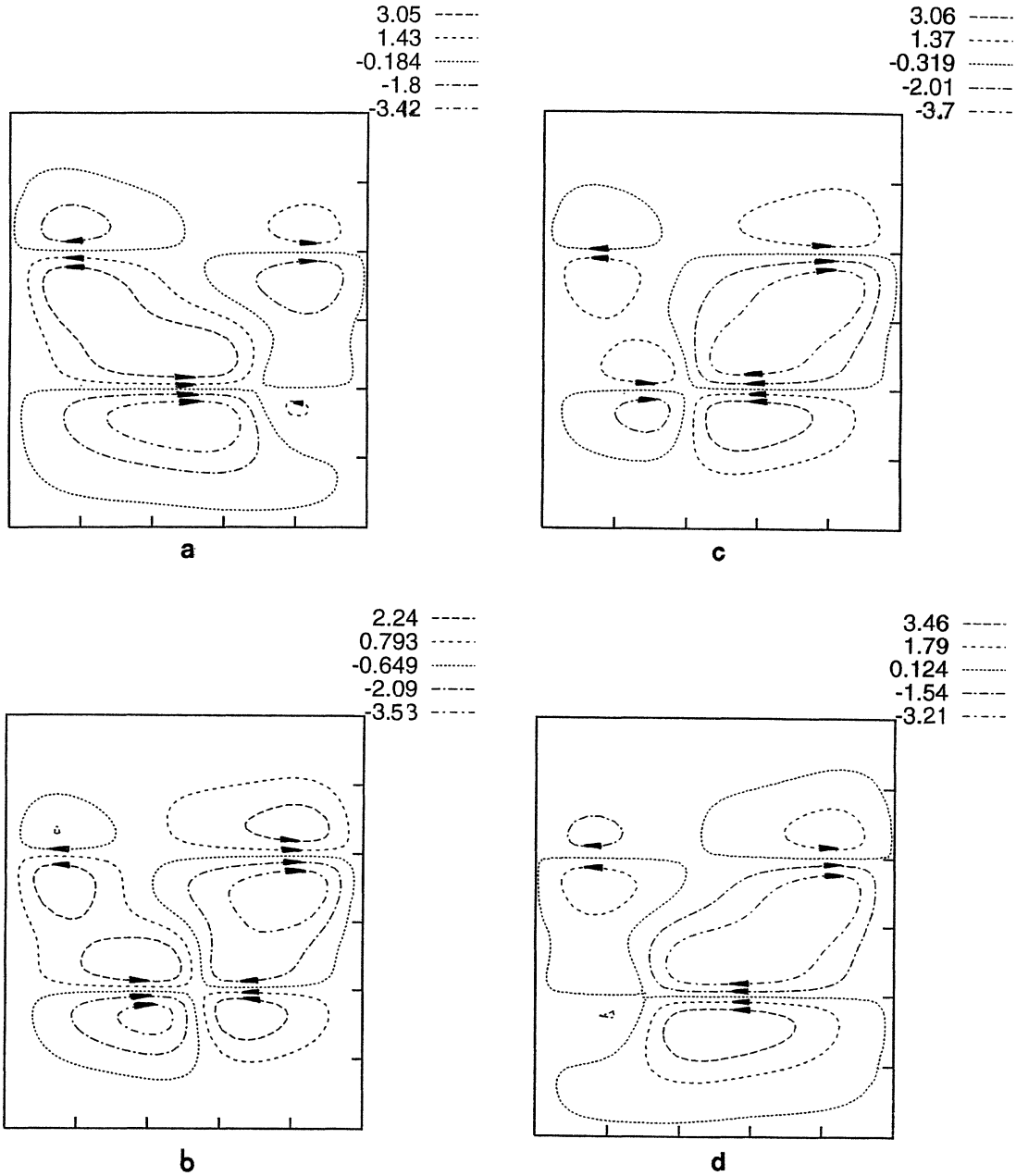

Figure 13. Streamlines for the periodic oscillatory motion for the half of the period ($M = 27500$, $G = 4500$, $\alpha = 200$).

realized (see *figure 10*, region II). We would like to emphasize that even in this situation, when for pure anticonvection ($G \neq 0$, $M = 0$) and for pure thermocapillary convection ($M \neq 0$, $G = 0$) only the steady motion takes place, the combined action of both mechanisms of instability may lead to the appearance of oscillations. The dependence $\tau(M)$ for different values of the Grashof number (line 2 (for the region I) and lines 3–6 (for the region II)) is shown in *figure 8*. The dependence $S_{il}(t)$ $(i = 1, 2, 3)$ for the region II is presented in *figure 12*. One can see that only S_{1l} changes the sign during the oscillatory process. The evolution of streamlines during one half of the period is shown in *figure 13*. During the second half of the period, the following property holds:

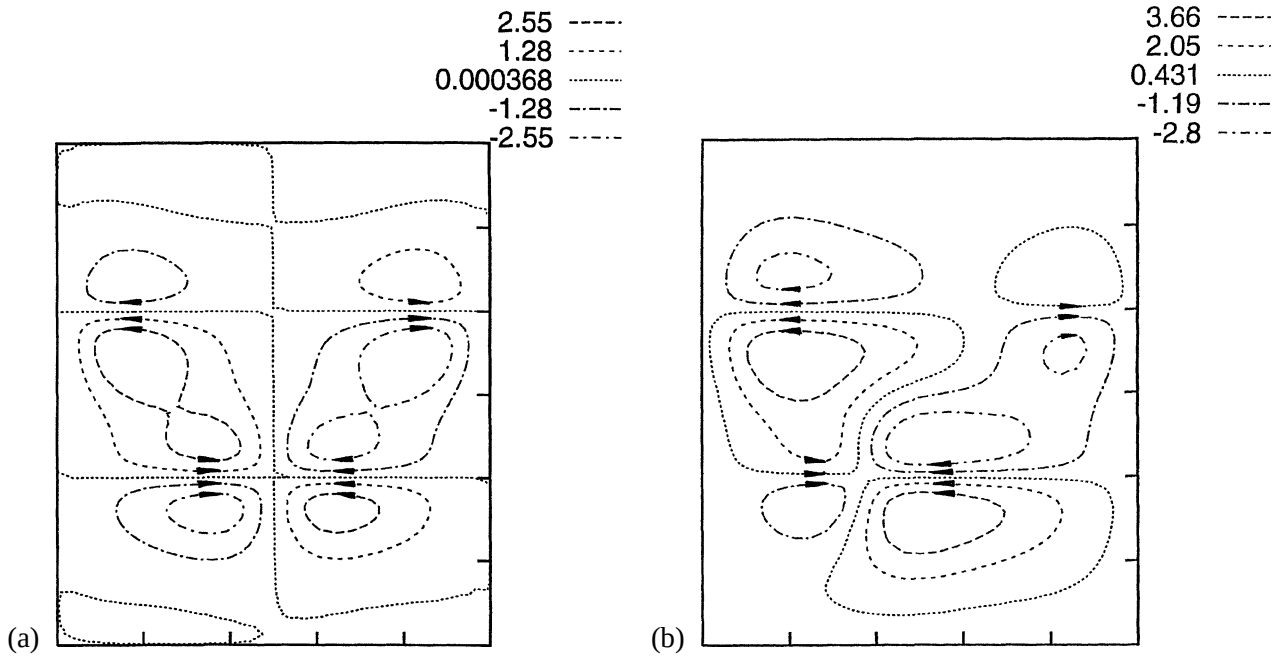

Figure 14. Streamlines for the steady motion ($M = 25000$, $\alpha = 200$): (a) $G = 4500$; (b) $G = 3000$.

$$\psi(x, t + \tau/2) = -\psi(-x, t), \qquad T(x, t + \tau/2) = T(-x, t).$$

The most intensive motion takes place mainly near the lower interface.

The physical origin of oscillations, in our opinion, is the competition between two possible, essentially different structures of the motion corresponding to *figures 9* and *11*. Because of this competition, both kinds of stationary structures are unstable. The oscillatory flow is some kind of a nonlinear superposition of both structures, and during the part of the period it resembles the first structure (*figures 13(a), 13(d)*) or the second structure (*figure 13(b)*).

For a fixed value of the Marangoni number the decrease in the Grashof number can lead to the establishment of two different steady states, depending on initial conditions (see *figures 14(a), 14(b)*). The motion shown in *figure 14(a)* is perfectly symmetric: the stream function and the temperature fields satisfy the symmetry conditions (11). For the motion shown in *figure 14(b)* the symmetry properties (11) are violated. The stability regions of oscillatory and steady motions (see *figure 10*, region III) overlap.

4. Conclusion

We considered the system of three immiscible viscous fluids with undeformable interfaces filling a closed cavity when heating is from above. Direct and indirect interactions of anticonvective and thermocapillary mechanisms of instability are studied. The specific new type of convective oscillations, essentially connected with the indirect interaction of both mechanisms of instability is found. It is shown that even in the situation, when for pure anticonvection and for pure thermocapillary convection only the steady motion takes place, the combined action of both mechanisms of instability may lead to the appearance of oscillations. The stability regions of oscillations and stationary motions overlap.

Acknowledgements

This work was partially supported by the German–Israeli Foundation for Scientific Research and Development, Research Contract #I 0460-228.10/95. The author acknowledges the support of the Israeli Ministry of Science and Humanities and the Israeli Ministry for Immigrant Absorption. The author thanks A. Nepomnyashchy and D. Kessler for useful advice and L. Shtilman for encouragement.

References

[1] Gershuni G.Z., Zhukhovitskii E.M., Convective Stability of Incompressible Fluid, Nauka, Moscow, 1972 (in Russian); English translation: Keter, Jerusalem, 1976.
[2] Welander P., Convective instability in a two-layer fluid heated uniformly from above, Tellus 16 (1964) 349.
[3] Gershuni G.Z., Zhukhovitskii E.M., On the stability of a horizontal layer system of immiscible fluids when heating from above, Izv. AN SSSR. Mekh. Zhidk. i Gaza 6 (1980) 26 (in Russian); Fluid Dynamics 15 (1980) 816.
[4] Simanovskii I.B., Convective stability of two-layer system, Avto-ref. cand. diss., Leningrad State University, 1980 (in Russian).
[5] Gershuni G.Z., Zhukhovitskii E.M., Simanovskii I.B., On stability and finite-amplitude motions in a two-layer system heated from above, Convective Flows, Perm, 3–11, 1981 (in Russian).
[6] Pearson J.R., On convective cells induced by surface tension, J. Fluid Mech. 4 (1958) 489–500.
[7] Sternling C.V., Scriven L.E., Interfacial turbulence: hydrodynamic instability and the Marangoni effect, AICHE J. 56 (1959) 514–523.
[8] Palmer J.J., Berg J.C., Hydrodynamic stability of surfactant solutions, heated from below, J. Fluid Mech. 51 (1972) 385–402.
[9] Nepomnyashchy A.A., Simanovskii I.B., Thermocapillary convection in a two-layer system, Fluid Dyn. Res. 18 (1983) 629–633.
[10] Simanovskii I.B., Convection at the combined action of non-Rayleigh and thermocapillary mechanisms of instability in a two-layer system heated from above, Convective Flows, Perm, 3–8, 1991 (in Russian).
[11] Simanovskii I.B., Nepomnyashchy A.A., Colinet P., Legros J.-C., Van Vaerenbergh S., The combined influence of anticonvective and thermocapillary mechanisms on the stability of systems with interface, in: Proc. VIII European Symposium on Materials and Fluid Sciences in Microgravity, Brussels, Belgium, ESA SP-333, 1992, pp. 767–770.
[12] Simanovskii I., Georis Ph., Hennenberg M., Van Vaerenbergh S., Wertgeim I., Legros J.-C., Numerical investigation on Marangoni–Benard instability in multi-layer systems, in: Proc. VIII European Symposium on Materials and Fluid Sciences in Microgravity, Brussels, Belgium, ESA SP-333, 1992, pp. 729–734.
[13] Liu Q.S., Roux, Instability of thermocapillary convection in multiple superposed in immiscible liquid layers, in: Proc. VIII European Symposium on Materials and Fluid Sciences in Microgravity, Brussels, Belgium, ESA SP-333, 1992, pp. 735–740.
[14] Georis Ph., Hennenberg M., Simanovskii I., Nepomnyashchy A., Wertgeim I., Legros J.-C., Thermocapillary convection in multilayer system, Phys. Fluids A 31 (1993) 1575–1582.
[15] Georis Ph., Contribution à l'étude des instabilités de Marangoni–Benard et Rayleigh–Benard pour les systèmes multicouches, Doctoral Thesis, Université Libre de Bruxelles, 1994.
[16] Simanovskii I.B., Anticonvective, steady and oscillatory mechanisms of instability in three-layer systems, Physica D 102 (1997) 313–327.
[17] Simanovskii I.B., Nepomnyashchy A.A., Convective Instabilities in Systems with Interface, Gordon & Breach, London, 1993, p. 279.
[18] Kuskova T.V., Chudov L.A., On approximate boundary conditions for vortex at calculation of the flows of viscous incompressible fluid, Comp. Meth. and Programming 11 (1968) 27 (in Russian).